Modelling and dynamic behavior of a vibratory roller for soil compacting based on lumped-parameter method

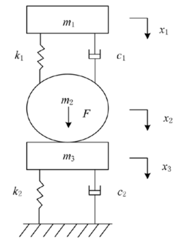

Modelización y comportamiento dinámico de un rodillo vibratorio para la compactación del suelo basado en el método de parámetros concentrados

Yang Wang[1,2], Fan Bai[3,*], Shaohua Li[1] and Yuelei Yang[1]

[1] State Key Laboratory of Mechanical Behavior and System Safety of Traffic Engineering Structures, Shijiazhuang Tiedao University, 050043, 17 East Road, Second North Ring, Shijiazhuang, P. R. China
[2] Center for Transportation Infrastructure Systems, The University of Texas at El Paso, 500 West University Avenue, El Paso, Texas, United States
[3] School of Traffic and Transportation, Shijiazhuang Tiedao University, 050043, 17 East Road, Second North Ring, Shijiazhuang, P. R. China
[*] Corresponding author, email: bf@stdu.edu.cn

DOI: http://dx.doi.org/10.6036/9867 | Received: 05/06/2020 • Reviewing: 23/06/2020 • Accepted: 07/10/2020

RESUMEN

- La interacción entre un rodillo y el suelo es un problema dinámico complejo que se ha convertido en un importante requisito teórico que limita el diseño de los rodillos y la aplicación de un rodillo avanzado en el desarrollo de la inteligencia y la informatización en la industria de los rodillos. Para aclarar el mecanismo de interacción entre un rodillo y el suelo durante el proceso de compactado, se estableció un modelo de dos grados de libertad (DOF) de parámetros concentrados para un sistema de acoplamiento vibratorio entre el rodillo y el suelo, teniendo en cuenta el estado de contacto entre el suelo y el rodillo. Sobre la base de la ecuación dinámica del sistema, los efectos del suelo y la fuerza de excitación en el comportamiento dinámico del rodillo se revelaron mediante la introducción de ciertos parámetros. Los resultados muestran que las frecuencias naturales del sistema aumentan obviamente desde el principio hasta la etapa intermedia de compactado, pero las frecuencias naturales sólo tienen ligeros aumentos después de la etapa intermedia de compactado, mientras el tambor permanece en contacto con el suelo. En comparación con la etapa inicial y la etapa intermedia, se puede observar que las frecuencias naturales primera y segunda aumentan 0,29 veces y 0,43 veces, respectivamente. Con el aumento de la compactación del suelo, aumenta la posibilidad de que el estado de vibración del rodillo pase de la estabilidad al caos. El aumento de la frecuencia de la fuerza de excitación y la disminución de la amplitud de la fuerza de excitación pueden mejorar eficazmente la vibración del sistema, y el comportamiento dinámico del sistema es más sensible a la frecuencia. El modelado y el análisis dinámico de un rodillo vibratorio se presentan en este estudio. El modelo puede utilizarse para el análisis teórico del reconocimiento de la vibración del rodillo, y las conclusiones proporcionan una referencia para el diseño y la aplicación de un rodillo.
- **Palabras clave:** Rodillo vibratorio, Modelo de parámetros concentrados, Comportamiento dinámico.

ABSTRACT

The interaction between a roller and soil is a complex dynamic problem that has become an important theoretical requirement constraining roller design and the application of an advanced roller in the development of intelligence and informatization in the roller industry. To clarify the interaction mechanism between a drum and soil during the rolling process, a two-degree-of-freedom (DOF) lumped-parameter model for a vibratory roller-soil coupling system was established with consideration of the contact state of the soil and the drum. Based on the dynamic equation of the system, the effects of the soil and the excitation force on the dynamic behavior of the roller were revealed by introducing certain parameters. The results show that the natural frequencies of the system increase obviously from the beginning to the intermediate rolling stage, but the natural frequencies have only slight increases after the intermediate rolling stage, while the drum stays in contact with the soil. Compared with the beginning stage and the intermediate stage, it can be found that the first and second natural frequencies increase by 0.29 times and 0.43 times, respectively. With the increase of the soil compactness, the possibility of the vibration state of the roller changing from stability to chaos increases. Increasing the frequency of the excitation force and decreasing the amplitude of the excitation force can effectively improve the vibration of the system, and the dynamic behavior of the system is more sensitive to the frequency. The modeling and dynamic analysis of a vibratory roller are presented in this study. The model can be used for the theoretical analysis of the vibration recognition of the roller, and the conclusions provide a reference for the design and application of a roller.

Keywords: Vibratory roller, Lumped-parameter model, Dynamic behavior.

1. INTRODUCTION

A roller is an engineering machine whose main purpose is to increase the bearing capacity of the soil, and rollers are especially suitable for major projects with high compaction quality demands and short-term construction conditions. In particular, vibratory rollers have become typical representatives of soil compaction equipment due to their excellent working efficiency [1]. By employing a rotating or reciprocating mass, an excitation force is applied to the drum of a vibratory roller, which makes the soil of the lift in high-frequency vibration, forcing the soil particles to rearrange to increase compactness [2, 3].

In engineering practice, the soil is gradually compacted with multiple rolling processes. The physical and mechanical properties of soil are also changed throughout the processes, which results in the parameter changes of a roller-soil coupling system [4]. This means that even with the same excitation pattern, a roller-soil coupling system may show different states with the progress of rolling [5]. With respect to a drum, a system has five typical states [6]. The first state is continuous contact. This state occurs when soil is very soft or the excitation force is weak, and when a drum is in continuous contact with soil. The second state is partial uplift. In each cycle of excitation force, soil exerts a sufficiently large upward force on a drum so that the drum cannot maintain contact with the soil. This is the most efficient operation condition of a roller. The third state is double jump, which is not an acceptable operation condition. In this state, the force on a drum applied by soil is greater than that of partial uplift, so that the drum motion repeats with every second period of excitation. The fourth state is rocking motion. This kind of motion can be observed when a roller makes a pass on stiff soil. The longitudinal axis of a drum rock to the left and right, which reduces the handling of a roller. The last state is chaotic motion. When a drum is rolling on hardened soil with improper operating parameters, the vibration is no longer a periodic motion but rather a chaotic motion, which should also be avoided.

To maintain the best operation condition of a roller, the parameters of the roller need to be adjusted at different stages of compaction to adapt to the changes in the mechanical properties of soil. For a vibratory roller, the vibration frequency and amplitude, stiffness of the shocker absorber, damping of the damper, and the mass of the roller are several elements related to the vibration [7]. Of these parameters, the stiffness, the damping, and the mass of the roller cannot be changed in principle, so the vibration force can only be adapted by adjusting the vibration frequency or amplitude.

2. STATE OF THE ART

The lumped-parameter method is a classical method for the dynamic analysis of mechanical systems, which has been widely used in different fields [8]. A series of significant results have been achieved based on various lumped-parameter models. To analyze the complex random vibration compaction process of a vibratory roller, Gong et al. [9] established a six-degree-of-freedom (DOF) linear model for a vibratory roller with consideration of the vibration effect of part of the compacted soil. The dynamic behavior of the roller was analyzed and the influences of some parameters on the operating condition, compactness, and compaction efficiency were clarified. The lumped-parameter model has a wide range of applications in the dynamic analysis of a roller, not only for traditional vertical vibratory rollers but also for new oscillatory rollers. Pistrol et al. [10] conducted a dynamic analysis of an oscillatory roller based on a linear lumped-parameter model. The analysis showed the "8-shape" relationship between the horizontal acceleration and vertical acceleration of the drum and revealed the effect of soil stiffness on this relationship. Such linear models are able to provide reliable analyses of the interaction between a roller and soil, but because there are many nonlinear factors in an actual system, introducing nonlinearity to the lumped-parameter model is commonly used in research.

Researchers have established and applied relatively complex nonlinear models for various purposes. Imran et al. [11] established a nonlinear model for a vibratory roller and compacted material. Compared with the aforementioned linear model, the main feature of this model was that the compacted material was assumed to be a lumped element-based viscoelastic-plastic model on a rigid base. This model could not only emulate the vibration response of a drum during field compaction but also replicate the pass-by-pass densification process in field compaction. Van Susante et al. [12] established 3-DOF and 4-DOF models with non-linear soil elements to describe the loss of contact between a drum and soil, suggesting that the heterogeneous soil conditions significantly affected the transient response of a roller. These studies focused on the accurate description of the nonlinear mechanical behavior of soil, and the improvements for the roller model were not addressed.

Researchers have attempted to build more comprehensive roller models. Nguyen et al. [13, 14] established an 11-DOF, three-dimensional nonlinear model. This model could be used to analyze the vibration of a drum and study the pitch and roll vibration of a cab. Based on this model, Nguyen et al. analyzed the low-frequency vibration characteristics of a vibratory roller and compared the dynamic performance of traditional rubber mounts, hydraulic mounts, and pneumatic mounts. This type of model was more suitable for the analysis of the overall mechanical performance of a roller.

The finite element method (FEM) has also been widely employed in the analysis of the rolling process, and a series of meaningful research studies have been achieved. Kenneally et al. [15] established an interaction model for compacted soil and a drum. Based on a plane strain, dynamic, time-domain finite element analysis, they quantified the relationships between the soil parameters collected by a continuous compaction roller and the modulus and thickness of the compacted layers. Jahedi et al. [16] certificated the availability of FEM for the simulation of the frictional rolling contact of a cylindrical component on a graded coating, and they revealed the effects of relevant factors on the stress of a contact area during the rolling process. By employing a finite-difference time-domain method with a modified Kelvin-Voigt model, Herrera et al. [17] analyzed the effects of the thickness and stiffness of the soil layers on the vertical acceleration of a drum. In order to analyze the stresses, strains, void ratio, and dynamic response of the drum center, Paulmichl et al. [18] established an interaction model for an oscillatory roller and soil in which the nonlinear inelastic behavior of the soil was captured as a strain-enhanced hypoplastic constitutive model.

According to the idea of nondestructive testing (NDT), vibration signals acquired by testing instruments can reflect the internal state of structures [19, 20]. Based on this principle, for nearly 50 years, researchers have continuously worked to reveal the relationship between measured roller values and compactness [21, 22]. In general, it is difficult for the numerical simulation of FEM to give answers in real-time, and the lumped-parameter model is highly efficient in solution finding, which can meet the accuracy requirements of real-time dynamic analysis [17]. Therefore, the lumped-parameter method is more capable for the automatic adjustment of the operating parameters of a roller and machine-integrated compaction monitoring.

The rolling process based on a vibratory roller can theoretically be described as a rigid cylinder with a sine excitation force moving at low speed on an elastoplastic body. However, due to the diversity and complexity of actual conditions, there is currently no ideal answer in the mechanical engineering field. The establishment of an efficiency mechanical model that can reflect the contact state of a drum and soil to clarify the dynamic behavior mechanism of a roller-soil coupling system is one of the academic focuses in the field of theoretical research and equipment development. In this study, with consideration of the vibration effect of a part of the compacted soil, a lump-parameter model of the vibratory roller-soil coupling system is established, and the dynamic behavior of the system is simulated for certain operation conditions.

The rest of the paper is organized as follows. Section 3 describes the establishment of the lumped-parameter model of a vibratory roller-soil coupling system and the derivation of the system dynamics equations. Section 4 describes the analysis of the dynamic response of a roller with certain operation conditions and reveals the effects of the excitation force and the soil parameters on the roller-soil coupling system. Section 5 summarizes the study.

3. METHODOLOGY

3.1. LUMPED-PARAMETER MODEL FOR VIBRATORY ROLLER-SOIL

For the rolling process, a 2-DOF lumped-parameter model for vibratory roller-soil is established, as shown in Fig. 1. As shown in Fig. 1, the coordinate system is established along the vertical direction. The displacements of the frame, the drum, the soil are described by x_1 x_2, and x_3, respectively. The frame and the drum are considered to be the lumped masses, described by m_1 and m_2. The damping elements between the frame and the drum are simplified as a massless linear spring and a damper, with the spring stiffness and the damping described by k_1 and c_1, respectively. The soil is simplified as a "mass-spring-damper" model, and the corresponding parameters are described by m_3, k_2, and c_2. The excitation force F of the drum is a sine function with an amplitude of F_0 and a frequency of ω, expressed as $F_0 \sin \omega t$.

The contact force between the drum and the soil is described as F_c. It is assumed that no tensile stress is generated inside the soil, so the soil vibration is ignored when the contact of the drum and the soil is lost. Based on this assumption, the relationship between m_2 and m_3 can be described as: when $x_2 \geq 0$, $x_2 = x_3$ and $F_c \geq 0$, and when $x_2 < 0$, $x_3 = 0$ and $F_c = 0$.

The motion of the frame is affected by m_1, k_1, c_1, x_1, and x_2. The dynamic equation of the frame is

$$m_1\ddot{x}_1 + c_1(\dot{x}_1 - \dot{x}_2) + k_1(x_1 - x_2) = m_1 g \tag{1}$$

The motion of the drum depends on not only m_2, m_1, k_1, c_1, x_1, and x_2, but also on F and F_c. When m_2 and m_3 are in contact, the dynamic equation of the drum can be expressed as

$$(m_2 + m_3)\ddot{x}_2 + c_1(\dot{x}_2 - \dot{x}_1) + k_1(x_2 - x_1) = F_0 \sin \omega t + (m_2 + m_3)g \tag{2}$$

When the contact of the drum and the soil is lost, the dynamic equation of the drum can be expressed as

$$m_2\ddot{x}_2 + c_1(\dot{x}_2 - \dot{x}_1) + k_1(x_2 - x_1) = F_0 \sin \omega t + m_2 g \tag{3}$$

In summary, the dynamic equations of the system can be expressed as

$$\begin{cases} \begin{bmatrix} m_1 & 0 \\ 0 & m_2+m_3 \end{bmatrix}\begin{bmatrix} \ddot{x}_1 \\ \ddot{x}_2 \end{bmatrix} + \begin{bmatrix} c_1 & -c_1 \\ -c_1 & c_1+c_2 \end{bmatrix}\begin{bmatrix} \dot{x}_1 \\ \dot{x}_2 \end{bmatrix} + \begin{bmatrix} k_1 & -k_1 \\ -k_1 & k_1+k_2 \end{bmatrix}\begin{bmatrix} x_1 \\ x_2 \end{bmatrix} = \begin{bmatrix} m_1 g \\ F_0 \sin \omega t + (m_2+m_3)g \end{bmatrix}, & x_2 \geq 0 \\ \begin{bmatrix} m_1 & 0 \\ 0 & m_2 \end{bmatrix}\begin{bmatrix} \ddot{x}_1 \\ \ddot{x}_2 \end{bmatrix} + \begin{bmatrix} c_1 & -c_1 \\ -c_1 & c_1 \end{bmatrix}\begin{bmatrix} \dot{x}_1 \\ \dot{x}_2 \end{bmatrix} + \begin{bmatrix} k_1 & -k_1 \\ -k_1 & k_1 \end{bmatrix}\begin{bmatrix} x_1 \\ x_2 \end{bmatrix} = \begin{bmatrix} m_1 g \\ F_0 \sin \omega t + m_2 g \end{bmatrix}, & x_2 < 0 \end{cases} \tag{4}$$

3.2. NATURAL FREQUENCIES OF THE SYSTEM FOR THE CONDITION OF SOIL PARTICIPATING IN THE VIBRATION

The model shown in Fig. 1 has 2 DOF, so it has two natural frequencies, denoted by ω_1 and ω_2, and $\omega_1 < \omega_2$. When the drum stays in contact with the soil, the solution of the natural frequencies can be given as follows.

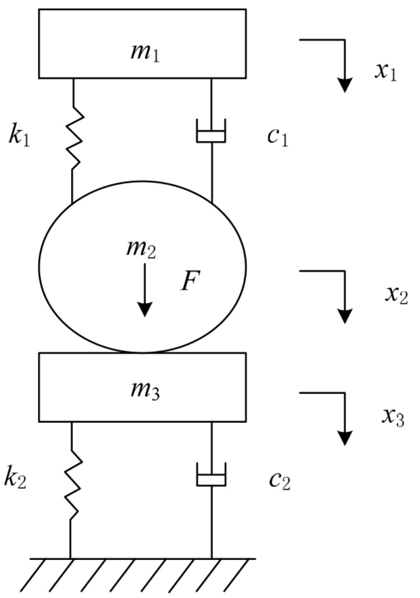

Fig. 1. Dynamic model of a vibratory roller-soil system

The free vibration equation of the system is

$$\begin{bmatrix} m_1 & 0 \\ 0 & m_2+m_3 \end{bmatrix}\begin{bmatrix} \ddot{x}_1 \\ \ddot{x}_2 \end{bmatrix} + \begin{bmatrix} k_1 & -k_1 \\ -k_1 & k_1+k_2 \end{bmatrix}\begin{bmatrix} x_1 \\ x_2 \end{bmatrix} = \begin{bmatrix} 0 \\ 0 \end{bmatrix} \tag{5}$$

If the equation has a non-zero solution, then the determinant of the characteristic equation is zero, that is

$$\begin{vmatrix} k_1 - m_1\omega^2 & -k_1 \\ -k_1 & k_1 + k_2 - (m_2+m_3)\omega^2 \end{vmatrix} = 0 \tag{6}$$

After solving Equation (6), the first natural frequency of the system is

$$\omega_1^2 = \frac{[k_1(m_1+m_2+m_3)+k_2 m_1] - \sqrt{[k_1(m_1+m_2+m_3)+k_2 m_1]^2 - 4m_1(m_2+m_3)k_1 k_2}}{2m_1(m_2+m_3)} \tag{7}$$

The second natural frequency is

$$\omega_2^2 = \frac{[k_1(m_1+m_2+m_3)+k_2 m_1] + \sqrt{[k_1(m_1+m_2+m_3)+k_2 m_1]^2 - 4m_1(m_2+m_3)k_1 k_2}}{2m_1(m_2+m_3)} \tag{8}$$

4. RESULT ANALYSIS AND DISCUSSION

4.1. MODEL PARAMETERS FOR SOME TYPICAL OPERATION CONDITIONS

The parameters of the system shown in Table 1 are given according to Literature 15. Three operation conditions are selected, corresponding to different stages of compaction. According to Literatures 15 and 23, the soil parameters of each operation condition are given as Table 2.

The two parameters related to the excitation force of the roller, F_0 and ω, are not constants. According to the range of F_0 given in Table 1, F_{0min} =1.58x10^4 N, F_{0max} =2.05x10^5 N, and F_{0mid} = (F_{0min} + F_{0max})/2=1.10x10^5 N are defined. Similarly, ω_{min} =125 rad/s, ω_{max} =220 rad/s, and ω_{mid}=(ω_{min}+ω_{max})/2=173 rad/s are defined. When the drum is in contact with the soil, it is assumed that m_3=0.3m_2.

Parameter	m_1 (kg)	m_2 (kg)	F_0 (N)	ω (rad/s)	k_1 (N/m)	c_1 (N·s/m)
Magnitude	2534	4466	1.58×10^4–2.05×10^5	125-220	6.02×10^6	4000

Table 1. Roller parameters

Operation condition	Compaction process	k_2 (N/m)	c_2 (N·s/m)
1	Beginning stage	1.40×10^7	7.00×10^4
2	Intermediate stage	4.68×10^7	4.00×10^4
3	Ending stage	5.68×10^7	2.00×10^4

Table 2. Soil parameters in different operation conditions

Operation condition	ω_1 (rad/s)	ω_2 (rad/s)
1	35	68
2	45	97
3	46	105

Table 3. Natural frequencies of the system in different operation conditions

4.2. EFFECT OF SOIL PARAMETERS ON THE SYSTEME

4.2.1. Impact on the natural frequency

During the rolling process, the changes in the stiffness and damping of the soil result in changes in the natural frequencies of the system. The natural frequencies of the system calculated with Equations (7) and (8) are listed in Table 3. The calculation results show that with the continuous compaction, the natural frequencies of the system increase. ω_1 increases from 35 rad/s to 46 rad/s, and ω_2 increases from 68 rad/s to 105 rad/s. The difference between the soil parameters in operation conditions 1 and 2 is considerably greater than the difference between operation conditions 2 and 3. The changes in the natural frequencies also show similar trends. From operation condition 1 to operation condition 2, ω_1 and ω_2 increase by 0.29 times and 0.43 times, respectively. From operation condition 2 to operation condition 3, ω_1 and ω_2 only increase by 0.02 times and 0.08 times, respectively. The calculation results show that with the transition from operation condition 1 to operation condition 3, ω_2 gradually approaches ω_{min}, which implies that in the intermediate and ending stages of the compaction process, for the excitation force with ω_{min}, violent vibration may have occurred for the drum.

4.2.2. Impact on the vibration amplitude of the roller

It is assumed that the drum is in continuous contact with the soil, and the effect of the change in soil parameters on the amplitude of the roller is discussed qualitatively. Although the assumption is arbitrary, for the theoretical analysis, this qualitative analysis still serves as a reference for the analysis of the vibration of the roller [24]. The lowest amplitude of excitation force is selected, F_0=1.58x10^4 N, and Equation (2) is used to calculate the system displacements in the different operation conditions. The amplitudes of x_1 and x_2 are described as X_1 and X_2, respectively. The amplitude-frequency responses of the system in different operation conditions are shown in Fig. 2 (see section: supplementary material).

Fig. 2 shows that the overall trends of the system response are essentially the same in different operation conditions. X_1 and X_2 exhibit resonance peaks at the first and second natural frequencies, respectively, which are determined by the inherent properties of the system. The maximum values of X_1 are obtained at the first resonance. The values are similar in the three operation conditions, at 0.0126 m, 0.0136 m, and 0.0121 m. The peak values of the second resonance are much smaller than the peak values of the first resonance, which are 0.0031 m, 0.0011 m, and 0.0015 m. To improve operating comfort, it is obvious that the vibration of the frame has to be reduced. Therefore, the frequency of the excitation force has to be selected as far away from the first natural frequency as possible.

Unlike X_1, the resonance peaks corresponding to the maximum values of X_2 are not similar in the different operation conditions. For operation condition 1, the maximum value of X_2, 0.0060 m, is obtained at the first resonance. The value of the second resonance peak is about half that of the first resonance peak, which is 0.0027 m. In operation conditions 2 and 3, the maximum values of X_2, 0.0034 m and 0.0057 m, are located at the second resonance peak. Between the first natural frequency and the second natural frequency, X_2 can be observed to be less than the static deformation, which is because part of the drum vibration is absorbed by the frame. The vibration absorption is determined by k_1 and c_1.

From the perspective of improving compaction efficiency, the frequency of the excitation force ω has to be set to a reasonable value to provide a higher X_2. Compared to the performance of X_1 and X_2, it can be concluded that ω has to be a value close to ω_2. By investigating the ω given in Table 1 and the ω_2 shown in Table 3, it can be determined that ω_2 is less than ω_{min}, and the difference in value between ω_2 and ω_{min} is kept reasonable to provide a higher X_2.

4.2.3. Impact on the vibration state of the drum

The effects of the soil stiffness and damping on contact state are discussed separately. The parameters of the excitation force are set to F_{0max} and ω_{min}. The soil damping during the rolling process is set as a constant at c_2=7.00x10^4 N·s/m. The soil stiffness k_2 increases from operation condition 1 to operation condition 3, that is, from 1.40x10^7 N/m to 5.68x10^7 N/m. Equation (4) is used to analyze the influence of the change of the soil stiffness on the vibration behavior of the drum. The bifurcation diagram of the drum is as shown in Fig. 3 (see section: supplementary material). As can be seen from Fig. 3, when k_2 is in the range of 1.40x10^7 N/m to 2.00x10^7 N/m, the system has a single period motion. When k_2=3.25x10^7 N/m, the system begins to have period doubling bifurcation. When k_2 increases to 3.38x10^7 N/m, chaos begins to appear in the system, indicating that in the intermediate and ending stages of compaction, the higher soil stiffness cannot guarantee a smooth response for the system.

Next, a similar method is used to analyze the effect of soil damping changes on the vibration behavior of the drum. The parameters of the excitation force are set to F_{0max} and ω_{max}. k_2 is maintained at 1.40x10^7 N/m. As c_2 decreases from 7.00x10^4 N·s/m to 2.00x10^4 N·s/m, the bifurcation diagram of the drum is as shown in Fig. 4 (see section: supplementary material). It can be seen from Fig. 4 that the overall trend of the vibration of the drum with the change of the parameters is similar to that shown in Fig. 3. When c_2 is in the range of 3.50x10^4 N·s/m to 7.00x10^4 N·s/m, the system has a single period motion. As c_2 decreases, no period doubling bifurcation occurs, and the single period motion gradually branches out and becomes chaotic motion.

Figs. 3 and 4 show that at certain roller parameters, as the soil parameters continue to change during the compaction process, with high stiffness and low damping appearing in the intermediate and ending stages of compaction, the motion of the drum appears to be chaotic vibration. For the chaotic vibration, the contact between the drum and the soil is difficult to maintain, which demonstrates the necessity of the use of the equation of motion given in Equation (4) to analyze the system response.

4.3. PARAMETER IMPACT ANALYSIS OF THE SYSTEM VIBRATION

4.3.1. Vibration of the system for a certain excitation pattern

To accurately recognize the motion of the system, numerical simulation results are presented here in the form of phase diagrams and the Poincare surface of sections. According to Table 1, the parameters of the excitation force are set to F_{0max} and ω_{min}. The responses of the frame and the drum in the three operation conditions are as shown in Figs. 5-8.

Figs. 5-8 show that in operation condition 1, the phase diagrams of the frame and the drum are regular ellipses, and each Poincare surface of the section appears as a single point. This indicates that in this mode, the system has a single period motion and the roller is in the normal operation condition. The vibration of the frame is more stable than that of the drum, and the frame and the drum differ by an order of magnitude in terms

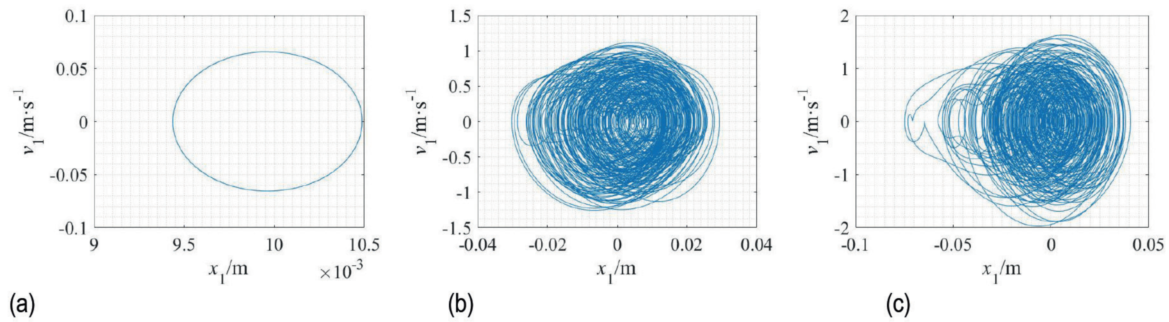

Fig. 5. Phase diagrams of the frame at F_{0max} and ω_{min} in different conditions. (a) Operation condition 1. (b) Operation condition 2. (c) Operation condition 3

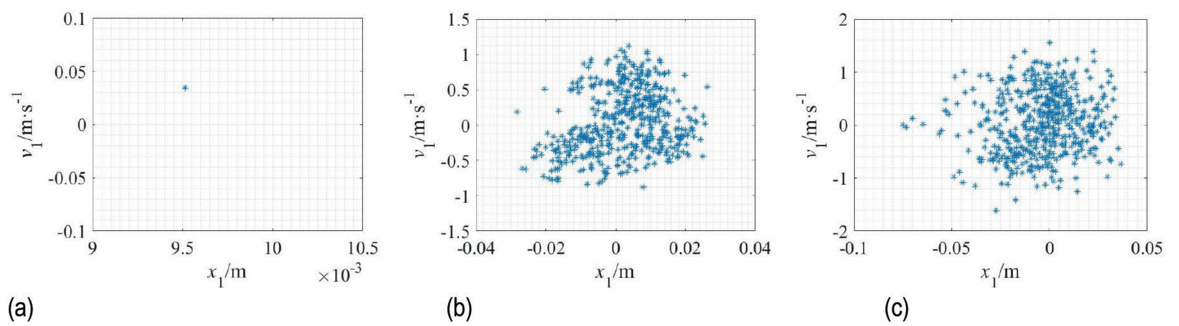

Fig. 6. Poincare surface of sections of the frame at F_{0max} and ω_{min} in different conditions. (a) Operation condition 1. (b) Operation condition 2. (c) Operation condition 3

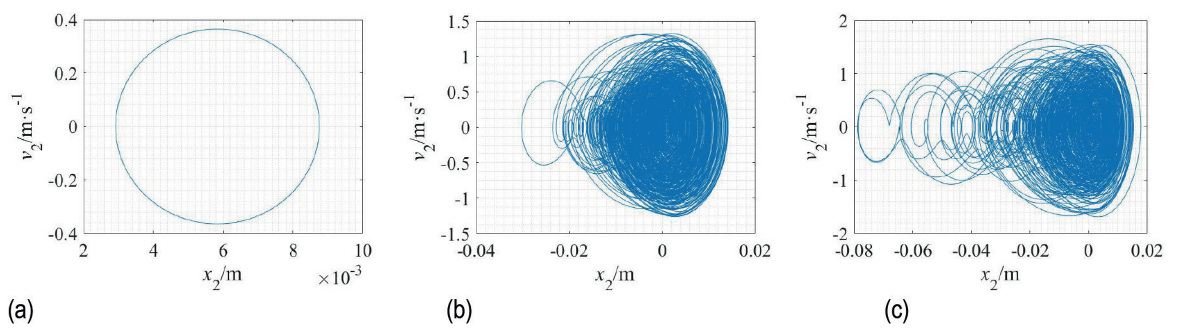

Fig. 7. Phase diagrams of the drum at F_{0max} and ω_{min} in different conditions. (a) Operation condition 1. (b) Operation condition 2. (c) Operation condition 3

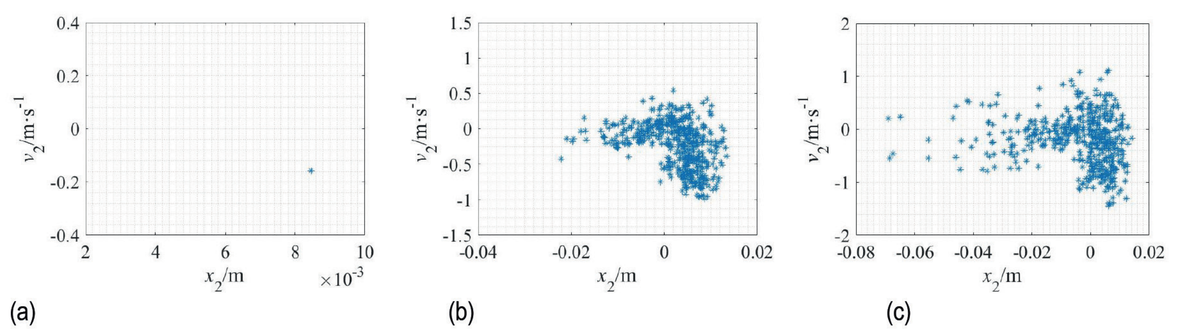

Fig. 8. Poincare surface of sections of the drum at F_{0max} and ω_{min} in different conditions. (a) Operation condition 1. (b) Operation condition 2. (c) Operation condition 3

of the displacement and speed. In operation conditions 2 and 3, the phase diagrams for the frame and the drum are confusing, and the Poincare surface of the sections appear as randomly scattered points. Obviously, with the given excitation pattern, the vibrations of the system in operation conditions 2 and 3 are both chaotic motions. As mentioned above, the chaotic vibration of the roller has to be avoided, and the system parameters need to be adjusted appropriately to ensure the normal operation of the roller.

4.3.2. Effect of the parameters of the excitation force on the system

Among the unfixed parameters of the system, the change of the soil parameters, which is the purpose of the compaction, is not avoidable. The only variable that can be actively adjusted is the excitation force. It has two parameters, the frequency ω and the amplitude F_0.

4.3.2.1. Effect of the frequency on the vibration of the system

$F_0 = F_{0max}$ is set in order to discuss the effect of the ω changes on the system. For operation condition 2, with the setting $\omega = \omega_{mid}$, the responses of the frame and the drum are as shown in Fig. 9 (see section: supplementary material). According to Fig. 9, it can be considered that the frame and the drum have a single period motion. The amplitude of the drum is $1.7x10^3$ m. Compared with the calculation results shown in Figs. 5-8, Fig. 9 fully illustrates the fact that the increased ω effectively suppresses the chaos of the system.

After setting the ω to ω_{mid} in the simulation of operation condition 3, the responses of the frame and the drum are as shown in Fig. 10 (see section: supplementary material). A comparison of the simulation results in Fig. 10 and Figs. 5-8 indicate that the vibration of the system is significantly improved overall, and the x_1 and x_2 ranges are reduced by an order of magnitude. Fig. 10 shows that the vibration of the drum is nearly a single period motion, and the vibration of the frame exhibits a significant bifurcation, indicating that the vibration of the drum is more sensitive to the excitation force. Despite the vibration of the frame being bifurcated, this state is acceptable in terms of the vibration intensity.

A higher value is arbitrarily set for ω, 200 rad/s, and the vibration response of the system is as shown in Fig. 11(see section: supplementary material). Obviously, the vibration of the system is further improved, and the vibration of the frame almost has a single period motion. However, judging from the values of x_1 and x_2, the effect of the parameter adjustment in this simulation is limited.

4.3.2.2. Effect of the amplitude on the vibration of the system

$\omega=\omega_{min}$ is set in order to discuss the effect of F_0 on the system. For operation condition 2, with the $F_0 = F_{0mid}$ setting, the responses of the frame and the drum are shown in Fig. 12 (see section: supplementary material). Fig. 12 shows that the vibration of the system is significantly improved. Although the frame and the drum do not have strictly single period motions, compared to Figs. 5-8, the values of x_1 and x_2 are greatly reduced, and this state is acceptable.

In operation condition 3, for the setting $F_0 = F_{0mid,}$ the response of the system is as shown in Fig. 13 (see section: supplementary material). Obviously, in this case, the vibrations of the frame and the drum are not improved dramatically, and significant chaotic motions are still exhibited. By comparing the calculation results shown in Fig. 9 and Fig. 13, it can be found that at the given parameters, the vibration of the system is more sensitive to the ω.

With F_0 reduced to $3.50x10^4$ N, the response of the system is as shown in Fig. 14 (see section: supplementary material). The results show that both the frame and the drum have single period motions. The vibration amplitude of the drum is $1.3x10^{-3}$ m. This shows that for the given soil parameters, within the normal parameters of the roller, the system can also be stabilized only by adjusting the amplitude of the excitation force.

5. CONCLUSIONS

To clarify the interaction mechanism between a roller and soil in the rolling process, and to reveal the influence of soil and the excitation force on the dynamic behavior of a roller, a linear lumped-parameter model for a vibratory roller-soil coupling system is established in this study. The model considers the contact state of the soil and the drum. By setting the parameters of some typical operation conditions for the model, the effects of the soil and the excitation force on the natural frequencies of the vibratory roller-soil coupling system are clarified. The conclusions are as follows.

(1) In normal operation conditions, the jump of the drum is normal and common, so the drum and the soil are not in continuous contact. To accurately analyze the vibration of the roller, it is necessary to select dynamic equations that account for the drum-soil contact state.

(2) The established vibratory roller-soil coupling model is a 2-DOF lumped-parameter model that has two natural frequencies. When ω_2 is kept at a reasonable value that is slightly less than ω_{min}, the roller can provide a higher compaction force. When the drum maintains continuous contact with the soil, the soil parameters have a significant effect on the natural frequency of the system. With the increase of compactness, the natural frequencies of the system increase. Compared with the intermediate and ending stages of the rolling process, the values of the soil parameters change more significantly in the beginning to the intermediate stage of the rolling process, which causes the natural frequencies of the system to experience corresponding significant change.

(3) Along with the compaction process, the ω_2 of the roller-soil coupling system gradually approaches ω_{min}. Therefore, at certain parameters, the continuous increase of compactness results in the motion of the roller changing from periodic to chaotic. In particular, in the intermediate and ending stages of the rolling process, higher soil stiffness cannot guarantee a smooth response of the system, and chaos may occur in the system.

(4) To avoid the occurrence of chaos, it is necessary to appropriately adjust the exciting force of the roller. In the beginning stage of compaction, an excitation force at a low frequency and a high amplitude has to be selected, and in the intermediate and ending stages of compaction, an excitation force at a high frequency and a low amplitude has to be selected. Increasing the frequency of the excitation force and decreasing the amplitude can effectively suppress the occurrence of chaos, and the system is more sensitive to the frequency. Compared with the frame, the vibration of the drum is affected more significantly by the excitation force.

The model established in this study can be used for the theoretical analysis of the vibration recognition of a roller. The conclusions can provide a reference for the design and application of a roller. Future research may focus on the application of the model for the vibration control of a roller in combination with field tests.

REFERENCES

[1] Ma J, Sun SZ, Rui HT, et al. "Review on China's road construction machinery research progress: 2018". China Journal of Highway and Transport. June 2018. Vol. 31-6. p.1-164

[2] Cacciola DV, Meehan CL, Baker III WJ, et al. "A comparison of continuous compaction control measurements with localized in situ test results". In International Foundation Congress and Equipment Expo 2018: Advances in Geomaterial Modeling and Site Characterization (GSP 295). March 2018. p.64-74. DOI: https://doi.org/10.1061/9780784481585.007

[3] Quynh LV, Thao VTP. "Study on influence of design parameters of drum's metal rubber isolation system of tandem vibratory roller on ride comfort". International Research Journal of Engineering and Technology. June 2019. Vol. 6. p.1647-1651

[4] Wersäll C, Nordfelt I, Larss S. "Soil compaction by vibratory roller with variable frequency". Géotechnique. March 2017. Vol. 67. p.272-278. DOI: https://doi.org/10.1680/jgeot.16.P.051

[5] Herrera C, Caicedo B. "Finite difference time domain simulations of dynamic response of thin multilayer soil in continuous compaction control". Procedia Engineering. September 2016. Vol. 143. p. 411-418. DOI: https://doi.org/10.1016/j.proeng.2016.06.052

[6] Pistrol J, Hager M, Adam D, et al. "Theoretical and experimental investigations of continuous compaction control (CCC) systems". In Proceedings of the 17th Nordic Geotechnical Meeting. May 2016. p. 865-872

[7] Quynh LV, Nguyen KT. "Optimal design parameters of cab's isolation system for vibratory roller using a multi-objective genetic algorithm." Applied Mechanics and Materials. January 2018. Vol. 875. p.105-112. DOI: https://doi.org/10.4028/www.scientific.net/amm.875.105

[8] Zarabadipour H, Yaghoubi Z. "Control of a non-holonomic mobile robot system with parametric uncertainty". Tehnički Glasnik -Technical Journal. November 2019. Vol. 13. p.43-50. DOI: https://doi.org/10.31803/tg-20190116100550

[9] Gong T, Liu BX. "Studies on dynamic parameters of intellectual vibratory roller". Advanced Materials Research. November 2012. Vol. 591-593. p.2024-2027. DOI: https://doi.org/10.4028/www.scientific.net/AMR.591-593.2024

[10] Pistrol J, Adam D. "Fundamentals of roller integrated compaction control for oscillatory rollers and comparison with conventional testing methods". Transportation Geotechnics. December 2018. Vol. 17 Part B. p.75-84. DOI: https://doi.org/10.1016/j.trgeo.2018.09.010

[11] Imran SA, Commuri S, Barman M, et al. "Modeling the dynamics of asphalt-roller interaction during compaction". Journal of Construction Engineering and Management. July 2017. Vol. 143-7. p.04017015. DOI: https://doi.org/10.1061/(ASCE)CO.1943-7862.0001293

[12] Van Susante PJ, Mooney MA. "Capturing nonlinear vibratory roller compactor behavior through lumped parameter modeling". Journal of Engineering Mechanics. August 2008. Vol. 134-8. p.684-693. DOI: https://doi.org/10.1061/(ASCE)0733-9399(2008)134:8(684)

[13] Nguyen V, Zhang J, Le V, et al. "Vibration analysis and modeling of an off-road vibratory roller equipped with three different cab's isolation mounts". Shock and Vibration. May 2018. Vol. 2018. p.8527574. DOI: https://doi.org/10.1155/2018/8527574

[14] Nguyen V, Zhang J, Yang X. "Low-frequency performance analysis of semi-active cab's hydraulic mounts of an off-road vibratory roller". Shock and Vibration. April 2019. Vol. 2019. p. 8725382. DOI: https://doi.org/10.1155/2019/8725382

[15] Kenneally B, Musimbi OM, Wang J, et al. "Finite element analysis of vibratory roller response on layered soil systems". Computers and Geotechnics. June 2015. Vol. 67. p.73-82. DOI: https://doi.org/10.1016/j.compgeo.2015.02.015

[16] Jahedi R, Adibnazari S. "Multi layered finite element analysis of graded coatings in frictional rolling contact". International Journal of Advanced Design and Manufacturing Technology. March 2015. Vol. 8-1. p.1-12

[17] Herrera C, Costa PA, Caicedo B. "Numerical modelling and inverse analysis of continuous compaction control". Transportation Geotechnics. December 2018. Vol. 17. p.165-177. DOI: 10.1016/j.trgeo.2018.09.012

[18] Paulmichl I, Furtmüller T, Adam C, et al. "Numerical simulation of the compaction effect and the dynamic response of an oscillation roller based on a hypoplastic soil model". Soil Dynamics and Earthquake Engineering. May 2020. Vol. 132. p.106057. DOI: https://doi.org/10.1016/j.soildyn.2020.106057

[19] Yang Y, Zhao W. "Curvelet transform-based identification of void diseases in ballastless track by ground-penetrating radar". Structural Control and Health Monitoring. January 2019. Vol. 26-4. p.e2322. DOI: https://doi.org/10.1002/stc.2322

[20] Nedoma J, Stolarik M, Kepak S, et al. "Alternative approaches to measurement of ground vibrations due to the vibratory roller: a pilot study". Sensors. December 2019. Vol. 19. p.5420. DOI: https://doi.org/10.3390/s19245420

[21] Meehan CL, Cacciola DV, Tehrani FS, et al. "Assessing soil compaction using continuous compaction control and location-specific in situ tests". Automation in Construction. January 2017. Vol. 73. p.31-44. DOI: https://doi.org/10.1016/j.autcon.2016.08.017

[22] Baker III WJ, Meehan CL. "Preliminary results from a continuous compaction control data set recorded during active earthwork construction". In Eighth International Conference on Case Histories in Geotechnical Engineering: Engineering Geology, Site Characterization, and Geophysics (GSP 311). March 2019. p.133-142. DOI: https://doi.org/10.1061/9780784482131.014

[23] Guo JW, Li J, Zhou ZL. "Detection and analysis of the degree of compaction of vibratory rollers". Construction Machinery. 2007. Vol. 8. p.86-89. DOI: https://doi.org/10.3969/j.issn.1001-554X.2007.08.027

[24] Niu ZP, Kan CZ. "Vibration jumping analysis of vibratory roller in continuous compaction quality testing". Water Resources and Hydropower Engineering. 2019. Vol. 50(S1). p.34-40. DOI: https://doi.org/10.13928/j.cnki.wrahe.2019.S1.007

APPRECIATION

This study was supported by the National Natural Science Foundation of China (Grant Nos. 11872255, 11972237, and 11972238).

SUPPLEMENTARY MATERIAL

https://www.revistadyna.com/documentos/pdfs/_adic/9867-1.pdf